Proceedings of the Twenty-sixth (2016) International Ocean and Polar Engineering Conference **www.isope.org**
Rhodes, Greece, June 26-July 1, 2016

ISBN 978-1-880653-88-3; ISSN 1098-6189

Numerical Computations of Spar Vortex-Induced Motions at Different Current Headings

*Weiwen Zhao, Decheng Wan**

State Key Laboratory of Ocean Engineering, School of Naval Architecture, Ocean and Civil Engineering, Shanghai Jiao Tong University, Collaborative Innovation Center for Advanced Ship and Deep-Sea Exploration, Shanghai, China
*Corresponding author

ABSTRACT

Vortex-induced motions (VIM) is a common phenomenon on varies kinds of deep-water offshore platforms such as deep draft semi-submersible and Spar. The present study investigates the VIM response of a Spar at different incident angles (current headings). The numerical investigations are conducted under supercritical Reynolds number using naoe-FOAM-SJTU, a solver developed based on the open source framework OpenFOAM. The self-developed six degree-of-freedom (6DoF) motion module and mooring system module are applied to model motions of Spar and the constraint of mooring lines, respectively. The shear stress transport (SST) based detached-eddy simulation (DES) is chosen for turbulence closure to predict the massive flow separation at high Reynolds number. The main purpose of this paper is to study the "hot spots" phenomenon of VIM response in a numerical way.

KEY WORDS: Vortex-induced motions; VIM; spar; incident angle; detached-eddy simulation; DES; hot spots.

NOMENCLATURE

A	Dynamic oscillation amplitude	(m)
A^*	$\sqrt{2}*RMS(A/D)$, nominal maximum	(-)
B	Linear damping of spring	(kg/s)
D	Diameter of spar hull	(m)
f_n	Natural frequency in still water	(Hz)
f_s	Vortex shedding frequency	(Hz)
H	Draft of spar hull	(m)
K	Spring stiffness	(N/s)
M	Mass of spar	(kg)
Re	Reynolds number	(-)
St	Strouhal number	(-)
U	Current velocity or towing velocity	(m/s)
U_r	U/f_nD, reduced velocity	(-)
λ	Scale ratio	(-)

INTRODUCTION

The original meaning of the word "spar" is a term for stout rounded pole used to support rigging as masts, booms, gaffs or yards. Spar platforms, as the name suggests, are offshore floating platforms which have columnar hulls and deep drafts. For decades, spars have been used as marker buoys and for gathering oceanographic data (Halkyard, 2015). It was not until the 1990s that the world's first oil and gas production spar platform named Neptune installed in the Gulf of Mexico. As of today, spars have evolved from classic spar, truss spar to cell spar. More recently, a new concept called "cell-truss" spar, which is a combination of cell spar and truss spar, was proposed by State Key Laboratory of Ocean Engineering (SKLOE) of Shanghai Jiao Tong University (Wang et al., 2008). Despite different design of varies kinds of spars, all these floating platforms have vertical hull form which is the main cause of vortex-induced motions (VIM). It is well known that when flow past bluff bodies, vortices are created and detached periodically from either side of the body. The vortex shedding of floating platforms results in periodical transverse forces and motions. Distinguished from vortex-induced vibrations (VIV), which is used to describe high frequency vibrations for long slender risers and pipes, the term "VIM" is for relatively low frequency motions of large floating objects. When the current velocity is in a specified range called "lock-in", vortex sheds at a frequency closed to the natural frequency of the structure, the VIM response amplitude becomes much larger as a result of resonance. To mitigate VIM response, spars are conventionally equipped with helical strakes. Well-optimized strakes configuration can reduce VIM response up to 85% (Dijk et al., 2003). While Dijk et al. at the same time pointed out due to the limitation of strakes, VIM can still occur at some certain current headings. Other experimental studies (Halkyard et al., 2005; Finnigan and Roddier, 2007; Zhang et al., 2011) also showed the strake effectiveness highly depend on current incident angles. The phenomena that spar VIM responses are unexpectedly high at some certain current directions are called "hot spots". Long time modular VIM response can cause mooring fatigue, even structural damage. This unique issue has become a research focus in the offshore engineering area.

Due to the complex geometry of the strakes and spar hull appurtenances (such as pipes, chains and anodes), it is nearly impossible to study VIM by using analytical methods. Thanks to the advance of computer science and fluid dynamics, Computational Fluid Dynamics (CFD), as the combination of the two, has been playing a more and more important role in numerical analyzing field. There have been a lot of publications of CFD analysis for spar VIM in recent years. All the researches take advantage of unsteady turbulence approaches, such as large-eddy simulation (LES) (Sirnivas et al., 2006; Zhao et al., 2014) or detached-eddy simulation (DES) (Halkyard et al., 2005; Thiagarajan et al., 2005; Atluri et al., 2006; Halkyard et al., 2006; Wang et al., 2008; Lefevre et al., 2013), rather than traditional (unsteady) Reynolds-average Navier-Stokes (URANS) model.

The main purpose of this paper is to investigate the "hot spots" of spar VIM in a numerical way. Spar VIM at different current headings under different reduced velocities are simulated and analyzed. Based on the numerical results, some meaningful conclusions are drawn.

NUMERICAL METHODS

Turbulence Modeling

The open source CFD toolbox OpenFOAM is well designed for its flexibility and extensibility and thus is chosen for simulations herein. The shear stress transport (SST) based detached-eddy simulation (DES) is implemented and applied for turbulence closure. DES was first proposed (Spalart et al., 1997) to take the great challenges of massively separated flows at high Reynolds numbers. It is a hybrid RANS/LES method which combines the best parts of RANS and LES, i.e., employs RANS model in near-wall regions to reduce grid cost and LES sub-grid scale model in other regions to better model the unsteady turbulent flow characteristics.

SST DES is a combination of Menter's SST RANS model (Menter, 1994) and LES sub-grid scale model. The formulation of SST DES adopted and implemented herein can be found in reference (Menter et al., 2003). The incompressible flow in SST DES model is governed by the continuity equation and momentum equations (namely Navier-Stokes equations).

$$\frac{\partial U_i}{\partial x_i} = 0 \tag{1}$$

$$\frac{\partial U_i}{\partial t} + \frac{\partial}{\partial x_j}\left(U_i U_j\right) = -\frac{\partial p}{\partial x_i} + \frac{\partial}{\partial x_j}\left(\left(\nu + \nu_t\right)\frac{\partial U_i}{\partial x_j}\right) \tag{2}$$

Where, U_i is the filtered or time-averaged velocity field, ν is the kinematic viscosity, ν_t is the eddy viscosity. Note that in OpenFOAM, the pressure for incompressible flow is normalized by density (i.e., pressure divide by density). To determine ν_t, two more equations are introduced

$$\frac{\partial k}{\partial t} + \frac{\partial (u_j k)}{\partial x_j} = \tilde{G} - \beta^* \omega k \cdot F_{DES} + \frac{\partial}{\partial x_j}\left[\left(\nu + \alpha_k \nu_t\right)\frac{\partial k}{\partial x_j}\right] \tag{3}$$

$$\frac{\partial \omega}{\partial t} + \frac{\partial (u_j \omega)}{\partial x_j} = \gamma S^2 - \beta \omega^2 + \frac{\partial}{\partial x_j}\left[\left(\nu + \alpha_\omega \nu_t\right)\frac{\partial \omega}{\partial x_j}\right] + \left(1 - F_1\right) CD_{k\omega} \tag{4}$$

The DES form is modified by multiplying the dissipation term by a coefficient F_{DES} in k-equation. Where, $\tilde{G} = \min\left(G, c_1 \beta^* k \omega\right)$, $G = \nu_t S^2$. F_1 is a blending function which is defined by

$$F_1 = \tanh\left\{\min\left[\max\left(\frac{\sqrt{k}}{\beta^* \omega y}, \frac{500\nu}{y^2 \omega}\right), \frac{4\alpha_{\omega 2} k}{CD^*_{k\omega} y^2}\right]^4\right\} \tag{5}$$

Where $CD^*_{k\omega} = \max\left(CD_{k\omega}, 10^{-10}\right)$, $CD_{k\omega} = 2\alpha_{\omega 2}\frac{1}{\omega}\frac{\partial k}{\partial x_j}\frac{\partial \omega}{\partial x_j}$. All constants in the above equations are obtained via $\phi = F_1\phi_1 + \left(1 - F_1\right)\phi_2$. After the k- and ω-equations are solved, the eddy viscosity can be calculated by

$$\nu_t = \frac{a_1 k}{\max(a_1 \omega, b_1 S F_2)} \tag{6}$$

In which, S is the invariant measure of the strain rate. F_2 is another blending function

$$F_2 = \tanh\left[\max\left(2\frac{\sqrt{k}}{\beta^* \omega y}, \frac{500\nu}{y^2 \omega}\right)^2\right] \tag{7}$$

All the constants required in equations can be found in Menter's paper (Menter et al., 2003).

The F_{DES} is defined as

$$F_{DES} = \max\left(\frac{L_t}{C_{DES}\Delta}\left(1 - F_S\right), 1\right) \tag{8}$$

Where, $L_t = \sqrt{k} / \left(\beta^* \omega\right)$ is the computed turbulent length scale, $\Delta = \sqrt[3]{\Delta x \Delta y \Delta z}$ is grid size, $C_{DES} = 0.61$ is DES constant, F_S is blending function which can be either F_1 or F_2, and $F_S = F_2$ is used in this paper.

Mooring System

The spar we trying to simulated is from a model test which was carried out by Chevron Energy Technology Company (CETC) (Finnigan and Roddier, 2007). In the towing experiments, the spar model is connected to the carriage using 4 lines of mixed cables and springs. While in CFD simulations we employ taut mooring lines to model the actual cables and springs. The line has an anchor point which is fixed during computation, and a mooring point which is moving with spar on hull. The origin length of mooring line can be calculated by the coordinate of two endpoints and the pretension of mooring line. In every time step, the coordinate of mooring point will be recalculated to obtain the new length. The mooring forces acted on spar are then computed by comparing the new length and original length for each mooring line.

Six-degrees-of-freedom motions

The solver naoe-FOAM-SJTU can handle any prescribed or predicted motions (Shen and Wan, 2013). The six-degrees-of-freedom (6DOF) motions of spar can be therefore obtained. Surge and sway are dominant motions at low Froude numbers, therefore in CFD simulations the free surface is not modeled and spar is constraint in the horizontal plane.

Dynamic Mesh Deformation

The dynamic mesh technique is respond for mesh motions. Grid cells will translate, stretch with the movement of hull boundary and keep the topology unchanged. The velocities of grid points are obtained by solving velocity Laplacian equation

$$\nabla \cdot (\gamma \nabla U_g) = 0 \tag{9}$$

In which, $\gamma = \frac{1}{r^2}$ is the diffusivity field which is quadratically the inverse distance of cell center to the nearest moving wall boundary. Once the grid velocities U_g are solved, the movement of grid points are then obtained by integrate grid velocity over time.

CASE AND CONDITIONS

The computational model in this paper is the towing model used by Finnigan and Roddier (2007). The model tests were carried out for hull equipped with partial and full appurtenances. While in the present study, all appurtenances are neglected for simplification, see Fig. 1. The main particulars of the model are listed in Table 1. The model is a hard tank section of a typical truss spar with a relatively large model scale (i.e. λ=1:22.3) such that all the towing cases are under super-critical Reynolds numbers conditions. This model was also used by Oakley Jr. and Constantinides (2007), Constantinides and Oakley Jr. (2013), as well as Lefevre et al. (2013) for further CFD benchmarking.

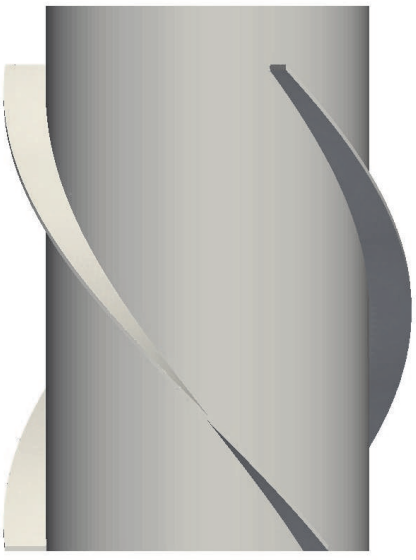

Fig. 1. Geometry of spar model

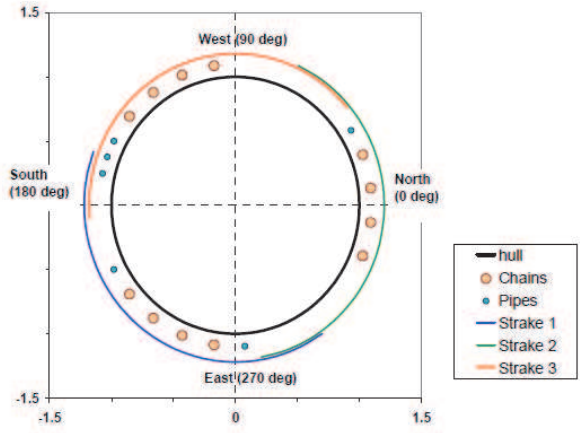

Fig. 2 Definition of current directions (Finnigan and Roddier, 2007)

Table 1. Main particulars of spar model

Parameter	Notation	Value
Scale ratio	λ	1:22.3
Diameter	D	1.75 m
Draft	H	2.95 m
Helical strakes		3 start, 13% D height 4 D pitch
Mass	M	7088 kg
Spring stiffness	K	2111 N/m
Linear damping	B	2.8 kg/s
Natural period of sway and surge	T_n	16.4 s

The conditions of CFD simulation are spar model subjected to uniform current. In order to investigate the "hot spots", three current directions are chosen considering the 3 start strakes design. The current direction definition is shown in Fig. 2. The reduced velocity is U_r=6-8, with corresponding current velocity U=0.640/0.746/0.853 m/s and Reynolds number Re=1.14/1.33/1.52×10^6. The cases conditions are listed in Table 2.

Table 2. Cases conditions

Case	Reduced velocity	Flow velocity (m/s)	Current heading (deg)	Re
1-3	6	0.640	30/60/90	1.14×10^6
4-6	7	0.746	30/60/90	1.33×10^6
7-9	8	0.853	30/60/90	1.52×10^6

The meshes used in this paper are generated by snappyHexMesh. It is an automatic polyhedral mesh generation tool utility provided by OpenFOAM. The mesh is generated based on a simple and orthogonal background mesh, splitting one hexahedral cell into 8 split-hexahedra cells and finally snap to the STL geometry. For different current incident angles, the STL geometry is first rotated and mesh is generated

by rerunning snappyHexMesh. The computational domain is defined as follows: $10D < x < 17D$, $-5D < y < 5D$ and $-3H < z < 0$. The mesh regions around hull surface and at wake are refined locally. The boundary layer meshes are extruded from hull surface to accurately model the near wall flow characteristics, see Fig. 3. The total mesh is approximately 900 000 polyhedral cells.

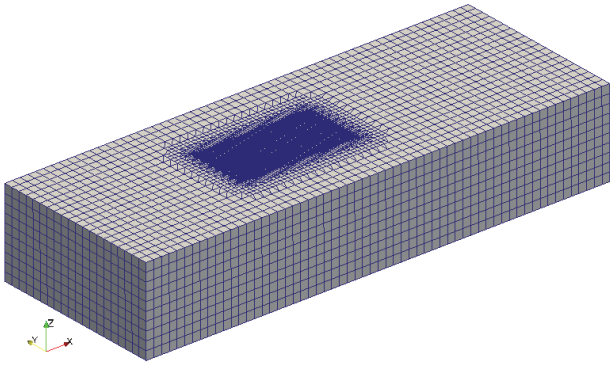

Fig. 3. Computational grid

The free decay test is performed first to verify the proper natural oscillation period of the system. The spar model is placed to about $0.25D$ away from the x-axis and allowed to oscillate freely without inflow. The oscillating period of the system in numerical test is about 15.6 seconds (Fig. 4). The sway & surge natural period measured in the experiments is 16.4 seconds.

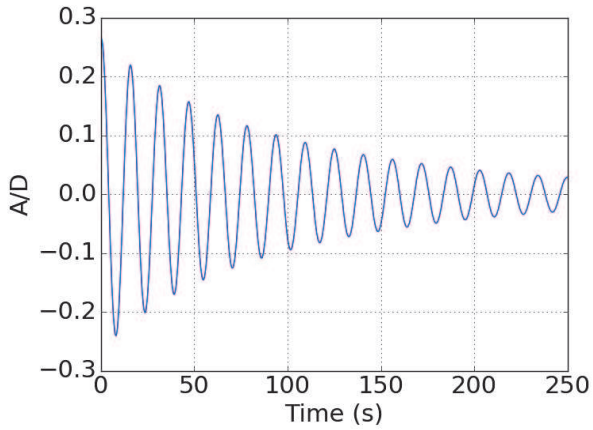

Fig. 4. Time history of sway for free decay test

All the calculations are carried out using the CFD solver naoe-FOAM-SJTU. The simulations were performed on a Linux cluster with 40 CPU cores, or 2 nodes which contains 20 CPU cores per node. The time step is 0.04s and is discretized with a 2nd order implicit scheme. 300 seconds which is corresponding to 18 vortex shedding cycles were calculated for each case.

RESULTS AND DISCUSSIONS

Oakley Jr. and Constantinides (2007) indicated that spar VIM is strongly modulated and the maximum of A/D is not appropriate to evaluate the motions. They proposed a term called "nominal maximum" which is defined as square root of 2 times root mean square (RMS) of non-dimensional motion time series or

$$A^* = \sqrt{2}\frac{1}{D}\sqrt{\frac{1}{N}\sum_{n=1}^{N}\left(A_n - \bar{A}\right)^2} \tag{10}$$

where, N is the number of sampling points, A_n is sway response at n-th sampling points, $\bar{A}$ is the averaged sway response.

Duplicate tests show that nominal maximum is highly repeatable with a difference under 0.05 (Oakley Jr. and Constantinides, 2007). While maximum of A/D is always varying among each towing test because of the unsteady characteristics of the system. It is therefore more robust and reliable to consider nominal maximum as a measure of VIM response than the maximum dimensionless amplitude.

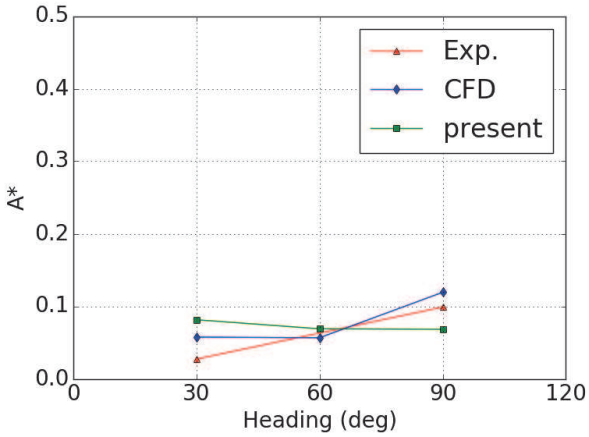

Fig. 5. VIM response at U_r=6 for different current headings

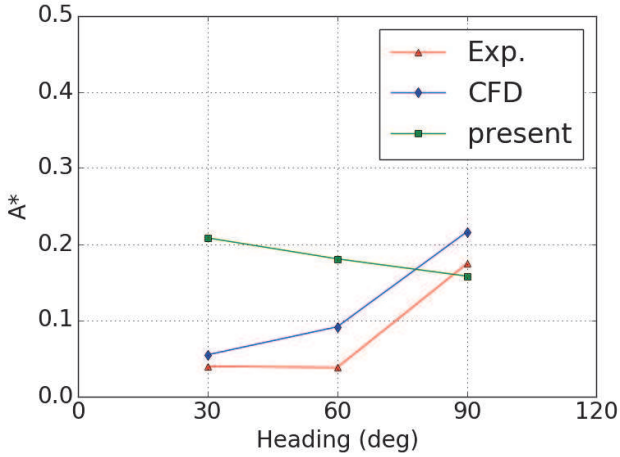

Fig. 6. VIM response at U_r=7 for different current headings

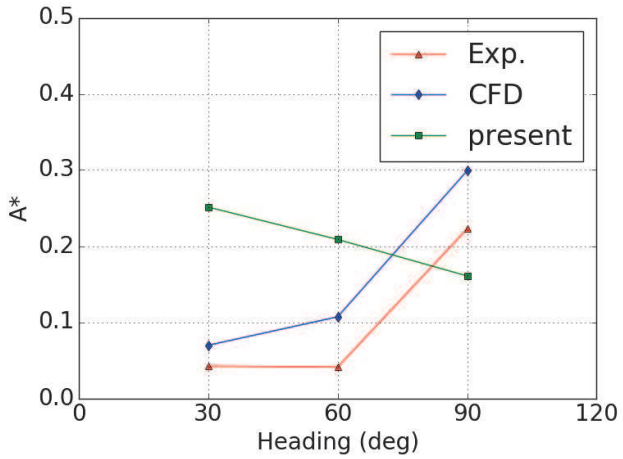

Fig. 7. VIM response at U_r=8 for different current headings

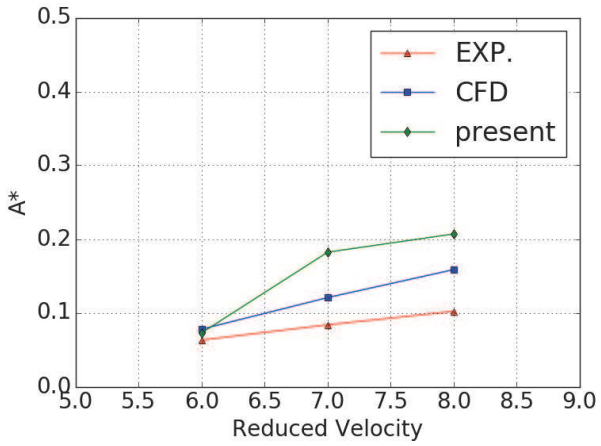

Fig. 8. Nominal maximum at different reduced velocities

Figs. 5-7 show the nominal maximum for spar at different reduced velocities. Red triangular markers represent the results of towing experiments performed by Finnigan and Roddier (2007). Blue diamond markers are the simulation results of Oakley Jr. and Constantinides (2007). Green square markers are present results. The transition sections at the beginning of the present numerical simulation is truncated in the calculation for nominal maximum. The variation tendency of nominal maximum between towing experiments and Oakley Jr.'s numerical results are consistent, while the present paper shows different results from the twos. At 30° and 60° headings, the present CFD overpredicts the VIM response. While at 90° heading, it is underpredicted by the current study. A finer grid was generated later and was used for simulation in order to address the issue, but the results didn't improve too much. One of the possible reasons is the explicit scheme for motion solver. In the current naoe-FOAM-SJTU solver, 6DoF motions are solved explicitly (Shen and Wan, 2013). The hydrodynamic, gravitational and mooring forces and moments used to solve 6DoF motion equations are obtained from the previous time step. For rigid body motions coupled with flows, the explicit motion solver is conditionally stable, depending on the time step of simulation. Later work applying a smaller time-step shows slightly different results comparing to the current larger time-step, indicating it is not a problem to solve motion using an explicit scheme. We believe this is attributed to the inaccurate geometry model. Small variation of current headings may lead to large difference of VIM response, i.e., the VIM response is very sensitive to the current headings. The fidelity of strakes and accurate definition of current headings are very important for numerical simulations of spar VIM. This has been pointed out in many opening literatures, see for instance, Chung et al. (1993; 1994) conducted a set of systematical experiments for vortex shedding of circular cylinder with and without helical strakes and their results show that different current incident angles will results in different drag and lift forces. Moreover, striking torsional deformation has been observed, which is caused by torsional moments.

In spite of the inaccurate nominal maximum for different current headings, the variation tendency at different reduced velocities are consistent with Finnigan's towing experiments and Oakley Jr.'s simulations, see Fig. 7. The system enters "lock-in" when reduced velocity is at the range of 6~8.

Fig. 9 and Fig. 10 illustrate the instantaneous vorticity iso-surface for U_r=6, current heading 30° and 90°, respectively. It can be clearly seen that the flow separation is mainly controlled by the helical strakes. In Fig. 9, flow separation also occurs at the side of spar hull, suggesting an extra transverse force acting on the spar. This may be the main reason of different VIM response between different current headings.

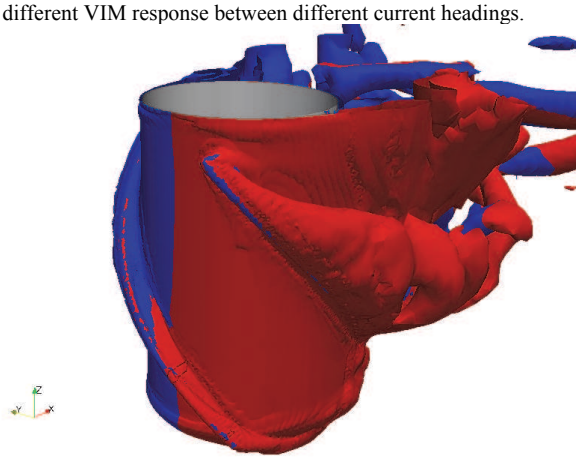

Fig. 9. Iso-surface of vorticity for U_r=6, heading 30°

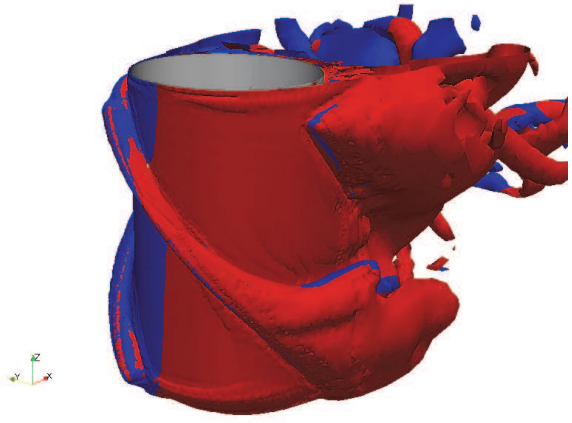

Fig. 10. Iso-surface of vorticity for U_r=6, heading 90°

CONCLUSIONS

This study tries to investigate the "hot spots" phenomenon of spar VIM under super-critical Reynolds numbers (above 10^5~10^6) in a numerical way and met with partial success. The present study failed to capture the "hot spots" current headings, which to the author's point of view, is attributed to the not detailed geometric model. Especially the fidelity of strakes and the definition for current headings. The reference for VIM towing model test (Finnigan and Roddier, 2007) did not give the detailed design and orientation of strakes (i.e., the thickness, start and end position of strakes). However, the reasons why different VIM responses to different current headings greatly depend on the detailed helical strakes geometry.

One of the minor concerns could be the explicit scheme of motion solver. For spar VIM, the simulation time should cover 25 oscillating cycles as suggested by Oakley Jr. and Constantinides (2007) and Lefevre et al. (2013). By switching to an implicit motion solver, the simulation is stable for larger time step and can reduce computational cost significantly. Another concern is the computational grids. In the current study, grids are regenerated for each current headings conditions. This is a large of repetitive work if the current conditions containing more angle subdivisions. A cylinder computational domain with special boundary conditions could be an effective alternative to reduce the duplication of work. These will be considered as the future work of the current study.

ACKNOWLEDGEMENTS

This work is supported by the National Natural Science Foundation of China (51379125, 51490675, 11432009, 51579145, 11272120), Chang Jiang Scholars Program (T2014099), Program for Professor of Special Appointment (Eastern Scholar) at Shanghai Institutions of Higher Learning (2013022), Innovative Special Project of Numerical Tank of Ministry of Industry and Information Technology of China (2016-23) and Foundation of State Ley Laboratory of Ocean Engineering (GKZD010065), to which the authors are most grateful.

REFERENCES

Atluri, S, Halkyard, J, and Sirnivas, S (2006). "CFD simulation of Truss Spar Vortex-Induced Motion," *Proc 25th Int Conf Offshore Mech Arct Eng - OMAE*, Hamburg, Germany.

Chung, JS, and Whitney, AK (1993). "Flow-Induced Moment and Lift for a Circular Cylinder with Cable Attachment," *Int J Offshore Polar Eng*, ISOPE, 3(04), 280–287.

Chung, JS, Whitney, AK, Lezius, D, and Conti, RJ (1994). "Flow-Induced Torsional Moment and Vortex Suppression for a Circular Cylinder with Cables," *Proc 4th Int Offshore Polar Eng Conf*, Osaka, Japan, ISOPE, 3, 447–459.

Constantinides, Y, and Oakley Jr., OH (2013). "Prediction and screening of truss spar vim with CFD," *Proc 32nd Int Conf Offshore Mech Arct Eng - OMAE*, Nantes, France, 7.

Dijk, RRT van, Magee, A, Perryman, S, and Gebara, J (2003). "Model test experience on vortex induced vibrations of Truss Spars," *Offshore Technol Conf*, Houston, Texas, USA.

Finnigan, T, and Roddier, D (2007). "Spar VIM model tests at supercritical reynolds numbers," *Proc 26th Int Conf Offshore Mech Arct Eng - OMAE*, San Diego, California, USA, 3, 731–740.

Halkyard, J (2015). "Large Spar Drilling and Production Platforms for Deep Water Oil and Gas," *Large Floating Structures*, Springer Singapore, 221–260.

Halkyard, J, Sirnivas, S, Holmes, S, Constantinides, Y, Oakley, O, and Thiagarajan, K (2005). "Benchmarking of truss spar vortex induced motions derived from CFD with experiments," *Proc 24th Int Conf Offshore Mech Arct Eng - OMAE*, Halkidiki, Greece, 3, 895–902.

Halkyard, J, Atluri, S, and Sirnivas, S (2006). "Truss spar vortex induced motions: Benchmarking of CFD and model tests," *Proc 25th Int Conf Offshore Mech Arct Eng - OMAE*, Hamburg, Germany.

Lefevre, C, Constantinides, Y, Kim, JW, Henneke, M, Gordon, R, Jang, H, and Wu, G (2013). "Guidelines for CFD simulations of spar VIM," *Proc 32nd Int Conf Offshore Mech Arct Eng - OMAE*, Nantes, France, 7.

Menter, FR (1994). "Two-equation eddy-viscosity turbulence models for engineering applications," *AIAA J*, 32(8), 1598–1605.

Menter, FR, Kuntz, M, and Langtry, R (2003). "Ten years of industrial experience with the SST turbulence model," *Turbul Heat Mass Transf*, 4(1), 625–632.

Oakley Jr., OH, and Constantinides, Y (2007). "CFD truss spar hull benchmarking study," *Proc 26th Int Conf Offshore Mech Arct Eng - OMAE*, San Diego, California, USA, 3, 703–713.

Shen, Z, and Wan, DC (2013). "RANS computations of added resistance and motions of a ship in head waves," *Int J Offshore Polar Eng*, 23(4), 263–271.

Sirnivas, S, Allain, O, Wornom, S, Dervieux, A, and Koobus, B (2006). "A study of LES models for the simulation of a turbulent flow around a truss Spar geometry," *Proc 25th Int Conf Offshore Mech Arct Eng - OMAE*, Hamburg, Germany.

Spalart, P, Jou, W, Strelets, M, and Allmaras, S (1997). "Comments on the feasibility of LES for wings, and on a hybrid RANS/LES approach," *Adv DNSLES*, 1, 4–8.

Thiagarajan, KP, Constantinides, Y, and Finn, L (2005). "CFD analysis of vortex-induced motions of bare and stroked cylinders in currents," *Proc 24th Int Conf Offshore Mech Arct Eng - OMAE*, Halkidiki, Greece, 3, 903–908.

Wang, Y, Yang, J, and Li, X (2008). "CFD analysis of unsteady flows around a new Cell-Truss Spar and the corresponding vortex-induced motions," *Proc 27th Int Conf Offshore Mech Arct Eng - OMAE*, Estoril, Portugal, 5, 567–575.

Zhang, H, Xiao, L, Lu, H, and Li, X (2011). "Experimental Investigation On Vortex Induced Motions of Truss SPARS," *Proc 21st Int Offshore Polar Eng Conf*, Maui, Hawaii, USA, ISOPE, 3, 1270–1275.

Zhao, W, Shen, Z, and Wan, DC (2014). "Numerical Investigation of the Vortex Induced Motion of SPAR in Uniform Current," *Proc 24th Int Ocean Polar Eng Conf*, Busan, Korea, ISOPE, 3, 362–367.